Physics Letters B 697 (2011) 254–259

Contents lists available at ScienceDirect

Physics Letters B

www.elsevier.com/locate/physletb

Chiral dynamics of the $S_{11}(1535)$ and $S_{11}(1650)$ resonances revisited

Peter C. Bruns [a], Maxim Mai [b,*], Ulf-G. Meißner [b,c]

[a] Institut für Theoretische Physik, Universität Regensburg, D-93040 Regensburg, Germany
[b] Helmholtz-Institut für Strahlen- und Kernphysik (Theorie) and Bethe Center for Theoretical Physics, Universität Bonn, D-53115 Bonn, Germany
[c] Institut für Kernphysik, Institute for Advanced Simulation, and Jülich Center for Hadron Physics, Forschungszentrum Jülich, D-52425 Jülich, Germany

ARTICLE INFO

Article history:
Received 10 December 2010
Accepted 2 February 2011
Available online 5 February 2011
Editor: J.-P. Blaizot

Keywords:
Pion–baryon interactions
Chiral Lagrangians
Baryon resonances

ABSTRACT

We analyze s-wave pion–nucleon scattering in a unitarized chiral effective Lagrangian including all dimension two contact terms. We find that both the $S_{11}(1535)$ and the $S_{11}(1650)$ are dynamically generated, but the $S_{31}(1620)$ is not. We further discuss the structure of these dynamically generated resonances.

1. Introduction

Pion–nucleon scattering has traditionally been the premier reaction to study the resonance excitations of the nucleon. In particular, in the S_{11} partial wave, one finds two close-by resonances at 1535 and 1650 MeV, which overlap within their widths of about 100 MeV. It was pointed out early in the framework of unitarized coupled-channel chiral perturbation theory [1] that this resonance might not be a three-quark (pre-existing) resonance but rather is generated by strong channel couplings, with a dominant $K\Sigma - K\Lambda$ component in its wave function. This analysis was extended in Ref. [2], where within certain approximations the effects of 3-body $\pi\pi N$ channels were also included. Further progress was made in Ref. [3], where the S_{11} phase shift was fitted from threshold to about $\sqrt{s} \simeq 2$ GeV together with cross section data for $\pi^- p \to \eta n$ and $\pi^- p \to K^0 \Lambda$ in the respective threshold regions. This led to a satisfactory description of the S_{11} phase and a reasonable description of the inelasticity up to the ηN threshold. Two poles were found corresponding to the $S_{11}(1535)$ and the $S_{11}(1650)$ resonances together with a close-by unphysical pole on the first Riemann sheet. More recently, it was pointed out in a state-of-the-art unitary meson-exchange model that there is indeed strong resonance interference between the two S_{11} resonances, as each of these resonances provides an energy-dependent background in the region of the other [4].

In view of these developments and our attempts to construct a unitary and gauge-invariant model for Goldstone boson photoproduction off nucleons based on coupled-channel unitarized chiral perturbation theory [5], we consider in this Letter the two s-waves S_{11} and S_{31} in pion–nucleon scattering. We work in the framework of a coupled-channel Bethe–Salpeter equation (BSE) including in the driving potential all local terms of second order in the chiral counting, thus going beyond the often used approximation of simply including the leading-order Weinberg–Tomozawa interaction. Further, we do not perform the often used on-shell approximation. Note that $K^- p$ scattering including such dimension two terms was already analyzed in a framework equivalent to the on-shell approximation of the Bethe–Salpeter equation in Refs. [6–8]. Our investigation is restricted to center-of-mass energies below 1.8 GeV, as required for the future meson photoproduction studies. As we will show, both resonances in the S_{11} partial wave are dynamically generated, even if the scattering data are fitted only up to $\sqrt{s} = 1.56$ GeV. Quite in contrast, the $S_{31}(1620)$ resonance is not generated by the coupled-channel dynamics. We also analyze the structure of the dynamically generated resonances as revealed through their coupling to the various meson–baryon channels.

2. Formalism

We consider the process of meson–baryon scattering at low energies. The s-wave interaction near the thresholds is dominated by the Weinberg–Tomozawa contact term, derived from the effective chiral Lagrangian

$$\mathcal{L}_{\phi B}^{(1)} = \langle \bar{B}\left(i\gamma_\mu D^\mu - m_0\right)B\rangle + \frac{D/F}{2}\langle \bar{B}\gamma_\mu\gamma_5\left[u^\mu, B\right]_\pm\rangle, \quad (1)$$

* Corresponding author.
E-mail address: mai@hiskp.uni-bonn.de (M. Mai).

0370-2693 © 2011 Elsevier B.V. Open access under CC BY license.
doi:10.1016/j.physletb.2011.02.008

where $\langle\cdots\rangle$ denotes the trace in flavor space, $D_\mu B := \partial_\mu B + \frac{1}{2}[[u^\dagger, \partial_\mu u], B]$, m_0 is the baryon octet mass in the chiral SU(3) limit, and D, F are the axial coupling constants. The relevant degrees of freedom are the Goldstone bosons described by the traceless meson matrix U,

$$U = \exp\left(i\frac{\phi}{F_0}\right),$$
$$\phi = \sqrt{2}\begin{pmatrix} \frac{\pi^0}{\sqrt{2}} + \frac{\eta}{\sqrt{6}} & \pi^+ & K^+ \\ \pi^- & -\frac{\pi^0}{\sqrt{2}} + \frac{\eta}{\sqrt{6}} & K^0 \\ K^- & \bar{K}^0 & -\frac{2}{\sqrt{6}}\eta \end{pmatrix}, \tag{2}$$

where F_0 is the meson decay constant in the chiral limit, and the low-lying baryons are collected in a traceless matrix

$$B = \begin{pmatrix} \frac{\Sigma^0}{\sqrt{2}} + \frac{\Lambda}{\sqrt{6}} & \Sigma^+ & p \\ \Sigma^- & -\frac{\Sigma^0}{\sqrt{2}} + \frac{\Lambda}{\sqrt{6}} & n \\ \Xi^- & \Xi^0 & -\frac{2}{\sqrt{6}}\Lambda \end{pmatrix}. \tag{3}$$

We set external currents to zero except for the scalar one, which is set equal to the quark mass matrix, $s = \mathcal{M} := \mathrm{diag}(m_u, m_d, m_s)$. We furthermore use

$$u^2 := U, \qquad u^\mu := iu^\dagger\partial^\mu u - iu\partial^\mu u^\dagger,$$
$$\chi_\pm := u^\dagger\chi u^\dagger \pm u\chi^\dagger u, \qquad \chi := 2B_0 s, \tag{4}$$

where the constant B_0 is related to the quark condensate in the chiral limit.

The Weinberg–Tomozawa contact term mentioned above stems from the covariant derivative $D_\mu B$, and is of first order in the chiral power counting. Most chiral unitary approaches restrict their meson–baryon potential to this interaction, which generates the leading contribution to the s-wave scattering lengths. This approach has been remarkably successful in many cases, see e.g. [1, 9–13]. However, at first chiral order, there are also the Born graphs, describing the s-channel and u-channel exchanges of an intermediate nucleon. The full inclusion of these graphs in the driving term of the Bethe–Salpeter equation leads to conceptional and practical difficulties, which have not yet been solved to the best of our knowledge: (i) Iteration of the s-channel exchange Born graphs will generate various contributions leading to a renormalization of the various baryon masses (and wave function renormalizations), which are usually set to their physical values in the loop functions of the chiral unitary approach. These contributions would thus have to be dropped. In view of a later application to photoproduction, such a non-perturbative treatment of s-channel exchanges leads to complications with gauge invariance because the self-energies are linked (via a Ward–Takahashi identity) to the electromagnetic baryon form factors, which would also have to be treated in a corresponding (non-perturbative) fashion. (ii) Iteration of the u-channel diagram, on the other hand, leads to all kinds of genuine multi-loop topologies, as there is no factorization into simple one-loop terms any more. The corresponding integral equation could only be solved numerically, e.g. by employing a Wick rotation and a four-momentum cutoff. Problems with gauge invariance would also occur here. In the literature, the u-channel Born diagrams were usually treated within some approximation which effectively reduced the solution of the BSE to products of one-loop terms, or included perturbatively to guarantee a matching to ChPT amplitudes up to a given order, see e.g. [14]. All these approximations, however, destroy the exact correspondence of the individual terms in the solution of the BSE to dimensionally regularized Feynman graphs, which is crucial in our approach to photoproduction. Therefore, we will approximate our interaction kernel by a sum of contact terms. To go beyond the simple Weinberg–Tomozawa potential, we shall include the full set of meson–baryon vertices from the second-order chiral Lagrangian. These terms may lead to sizeable corrections to the leading-order results, see e.g. the calculation of NNLO corrections on meson–baryon scattering lengths within SU(3) ChPT [15]. The pertinent Lagrangian density was first constructed in [16] and reads in its minimal form [17]

$$\begin{aligned}
\mathcal{L}_{\phi B}^{(2)} = {} & b_{D/F}\langle\bar{B}[\chi_+, B]_\pm\rangle + b_0\langle\bar{B}B\rangle\langle\chi_+\rangle \\
& + b_{1/2}\langle\bar{B}[u_\mu, [u^\mu, B]_\mp]\rangle \\
& + b_3\langle\bar{B}\{u_\mu, \{u^\mu, B\}\}\rangle + b_4\langle\bar{B}B\rangle\langle u_\mu u^\mu\rangle \\
& + ib_{5/6}\langle\bar{B}\sigma^{\mu\nu}[[u_\mu, u_\nu], B]_\mp\rangle + ib_7\langle\bar{B}\sigma^{\mu\nu}u_\mu\rangle\langle u_\nu B\rangle \\
& + \frac{ib_{8/9}}{2m_0}\big(\langle\bar{B}\gamma^\mu[u_\mu, [u_\nu, [D^\nu, B]]_\mp]\rangle \\
& + \langle\bar{B}\gamma^\mu[D_\nu, [u^\nu, [u_\mu, B]]_\mp]\rangle\big) \\
& + \frac{ib_{10}}{2m_0}\big(\langle\bar{B}\gamma^\mu\{u_\mu, \{u_\nu, [D^\nu, B]\}\}\rangle \\
& + \langle\bar{B}\gamma^\mu[D_\nu, \{u^\nu, \{u_\mu, B\}\}]\rangle\big) \\
& + \frac{i\,b_{11}}{2m_0}\big(2\langle\bar{B}\gamma^\mu[D_\nu, B]\rangle\langle u_\mu u^\nu\rangle \\
& + \langle\bar{B}\gamma^\mu B\rangle\langle[D_\nu, u_\mu]u^\nu + u_\mu[D_\nu, u^\nu]\rangle\big),
\end{aligned} \tag{5}$$

with the b_i the pertinent dimension-two low energy constants (LECs). The LECs $b_{0,D,F}$ are the so-called *symmetry breakers* while the b_i $(i = 1, \ldots, 11)$ are referred to as *dynamical* LECs.

The strict perturbative chiral expansion is only applicable at low energies. Moreover, it certainly fails in the vicinity of resonances. The purpose of the present work is the extension of the range of applicability of the low-energy effective theory by means of a coupled channel Bethe–Salpeter equation (BSE). Introduced in [18] it has been proven to be very useful both in the purely mesonic and in the meson–baryon sector [1,9–13]. In contrast to perturbative calculations this approach implements two-body unitarity exactly and in principle allows to generate resonances dynamically. Due to the exact correspondence of the Bethe–Salpeter scattering amplitude with an infinite sum of dimensionally regularized Feynman graphs, we can use our solution of the BSE as an extended vertex in a model amplitude for meson photoproduction and arrive at a natural and straightforward way to implement gauge invariance in a chiral unitary framework (for details on the construction principles, see [5]).

In this section we collect the necessary formalism of the Bethe–Salpeter approach. We denote the in- and outgoing meson momenta by q_1 and q_2, respectively. Moreover the overall four-momentum is given by $p = q_1 + p_1 = q_2 + p_2$, where p_1 and p_2 are the momenta of in- and out-going baryon, respectively. For the meson–baryon scattering amplitude $T(\not{q}_2, \not{q}_1; p)$ and chiral potential $V(\not{q}_2, \not{q}_1; p)$ the integral equation to solve reads

$$\begin{aligned}
T(\not{q}_2, \not{q}_1; p) = {} & V(\not{q}_2, \not{q}_1; p) \\
& + i\int\frac{d^d l}{(2\pi)^d}V(\not{q}_2, \not{l}; p)S(\not{p} - \not{l})\Delta(l)T(\not{l}, \not{q}_1; p),
\end{aligned} \tag{6}$$

where S and Δ represent the baryon (of mass m) and the meson (of mass M) propagator, respectively, and are given by $iS(\not{p}) = i/(\not{p} - m + i\epsilon)$ and $i\Delta(k) = i/(k^2 - M^2 + i\epsilon)$. The BSE is depicted in Fig. 1.

So far we have suppressed the channel indices in the above formulas, however since we are dealing with coupled channels, T,

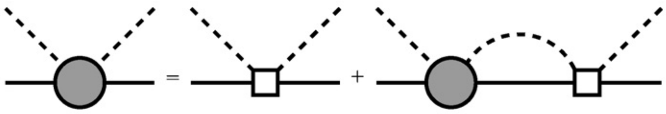

Fig. 1. Symbolical representation of the Bethe–Salpeter equation. Here the square and the circle represent the potential V and the scattering amplitude T, respectively.

V, S and Δ are matrices in channel space (the propagators are represented by diagonal matrices). In view of a later application to photoproduction off protons, we restrict ourselves to meson–baryon channels with strangeness $S=0$ and electric charge $Q=+1$. This leaves us with the following channels:

$$p\pi^0, \quad n\pi^+, \quad p\eta, \quad \Lambda K^+, \quad \Sigma^0 K^+, \quad \Sigma^+ K^0. \tag{7}$$

Now let us specify the interaction kernel to be iterated by means of Eq. (6). As explained above, we only include the contact-term contributions from $\mathcal{L}_{\phi B}^{(1)}$ and $\mathcal{L}_{\phi B}^{(2)}$ and omit the Born terms. To our knowledge this is the first time these NLO corrections of the chiral potential are included and unitarized within the full relativistic BSE, without making use of the on-shell approximation or s-wave projection of the chiral potential, so that also a p-wave is iterated. Separating the momentum space from channel space structures the chiral potential considered here takes the form:

$$\begin{aligned} V(\not{q}_2, \not{q}_1; p) = {} & A_{WT}(\not{q}_1 + \not{q}_2) \\ & + A_{14}(q_1 \cdot q_2) + A_{57}[\not{q}_1, \not{q}_2] + A_M(q_1 \cdot q_2) \\ & + A_{811}\big(\not{q}_2(q_1 \cdot p) + \not{q}_1(q_2 \cdot p)\big), \end{aligned} \tag{8}$$

where the first matrix only depends on the meson decay constants F_π, F_K, F_η, whereas A_{14}, A_{57}, A_{811} and A_M also contain the NLO LECs as specified in Appendix A. In going from the Lagrangian (5) to the above vertex rule, we have left out some terms which are formally of third chiral order.

The loop diagrams appearing in the BSE (6) are in general divergent and require renormalization. In case of a strict chiral perturbation expansion, the terms can be renormalized in a quite straightforward way, order by order, including at a given order of the calculation all the counterterms absorbing the loop divergences. On the other hand the treatment of the divergences of the BSE is known to be a complicated issue, see e.g. [5,19]. Although the unitarization of the chiral potential provides us with large benefits regarding dynamically generated resonances, it relies on approximations of the kernel, which destroy some fundamental features of quantum field theory, such as crossing symmetry.

There are various ways to treat the divergent integrals and the large baryon mass scale appearing. Without going into details here, we preserve the analytic structure of the loop integrals by utilizing dimensional regularization and just replacing the divergent part by a subtraction constant. The purely baryonic integrals are set to zero from the beginning. Thus, our treatment of the loop integrals is, in effect, similar to the EOMS regularization scheme advocated in [20]. As it was argued in [5] it is not possible to express the terms necessary to absorb the divergences in the BSE as counterterms derived from a local Lagrangian. However it is possible to alter the loop integrals in the solution of the BSE in a way that is in principle equivalent to a proper modification of the chiral potential itself (for an explicit demonstration, see Appendix F of [21]). In this spirit we apply the usual $\overline{MS}$ subtraction scheme, keeping in mind that the modified loop integrals are still scale-dependent. This regularization scale (μ) dependence would be canceled by the corresponding scale dependence of higher-order contact terms in the perturbative approach, but in our non-perturbative framework, the scale μ is used as a fitting parameter, reflecting the influence of higher-order terms not included in our potential. Note that in [3,19], the 12 loop integrals (4 for each meson–baryon, meson and baryon case) appearing there, gave rise to 12 finite subtraction constants, which were then also used as fitting parameters of their approach.

Having specified the kernel we are now ready to solve the Bethe–Salpeter equation. Given the structure of the kernel, its iteration via the BSE induces the following form of the scattering amplitude,

$$T(\not{q}_2, \not{q}_1; p) = \sum_{i=1}^{20} \aleph_i \cdot \mathrm{T}_i, \tag{9}$$

where the coefficients T_i are 6×6 matrices in channel space, which only depend on the center-of-mass energy $\sqrt{s}$ after fixing the LECs, and $\aleph := (\not{q}_1, \not{p}\not{q}_1, \not{q}_2\not{p}\not{q}_1, \not{q}_2\not{q}_1, \not{p}\not{q}_1(q_2 \cdot p), \not{q}_1(q_2 \cdot p), \not{q}_2(q_1 \cdot p), \not{q}_2\not{q}_1, (q_1 \cdot p)(q_2 \cdot p), \not{p}(q_1 \cdot p)(q_2 \cdot p), (q_1 \cdot p), \not{p}(q_1 \cdot p), (q_2 \cdot q_1), \not{p}(q_2 \cdot q_1), \not{q}_2\not{p}, \not{q}_2, \not{p}(q_2 \cdot p), (q_2 \cdot p), \mathbb{1}, \not{p})$ is a vector in the 20-dimensional space of invariant structures. Note that the scalar products are listed here as independent structures because we include the full off-shell dependence of the chiral potential in the BSE, which prevents us from writing them as simple functions of the Mandelstam variables s and t.

On the other hand the above decomposition allows us to pull the coefficients T_i out of the loop-integral in Eq. (6). Then these are fully determined by the solution of a linear system of equations in the space of invariant structures:

$$\mathrm{X}_{ij}\mathrm{T}_j = \mathrm{V}_i, \quad (i, j = 1, \ldots, 20), \tag{10}$$

where the V_i are coefficients of the chiral potential with respect to the invariant structures defined above and X is a 20×20 matrix. The latter connects different structures of the space of invariant structures via loop integrations on the r.h.s. of Eq. (6). Once the BSE has been solved, we can of course set the *external* four-momenta on their mass shells, leaving us with only two independent structures for the on-shell amplitude, i.e. $\mathbb{1}$ and $\not{p}$.

3. Results and discussion

Throughout the present work we use the following numerical values (in GeV) for the masses and the meson decay constants: $F_\pi = F_\eta/1.3 = 0.0924$, $F_K = 0.113$, $M_{\pi^0} = 0.135$, $M_{\pi^+} = 0.1396$, $M_\eta = 0.5478$, $M_{K^+} = 0.4937$, $M_{K^0} = 0.4977$, $m_p = 0.9383$, $m_n = 0.9396$, $m_\Lambda = 1.1157$, $m_{\Sigma^0} = 1.1926$ and $m_{\Sigma^+} = 1.1894$. The baryon mass in the chiral limit, m_0 in Eq. (5), can be fixed to 1 GeV without loss of generality, as any other value only amounts to a rescaling of the unknown LECs.

There are 17 free parameters in the present approach, given by the 14 LECs, as well as three subtraction constants for the regularized loop integrals, corresponding to the logarithms of the undetermined regularization scales (in GeV), i.e. $\log(\mu_\pi)$, $\log(\mu_K)$ and $\log(\mu_\eta)$. Here we take the regularization scale of each channel to be fixed by the respective meson, i.e. in addition to $\mu_{\pi N} =: \mu_\pi$ and $\mu_{\eta N} =: \mu_\eta$, we take $\mu_{K\Sigma} = \mu_{K\Lambda} =: \mu_K$. The latter constraint appears to be natural in view of our forthcoming work on meson photoproduction, where loops are present in which a photon-induced $\Lambda \to \Sigma^0$ transition occurs.

For the fits, we consider experimental data for s-wave πN scattering up to $W = 1.56$ GeV, i.e. partial wave amplitudes S_{11} and S_{31} (both real and imaginary parts) provided by the SAID-program at GWU, see [22]. Comparing an earlier analysis by the Karlsruhe group [23] to the current one, we assign for the energies below $W = 1.28$ GeV an absolute systematic error of 0.005 and for higher

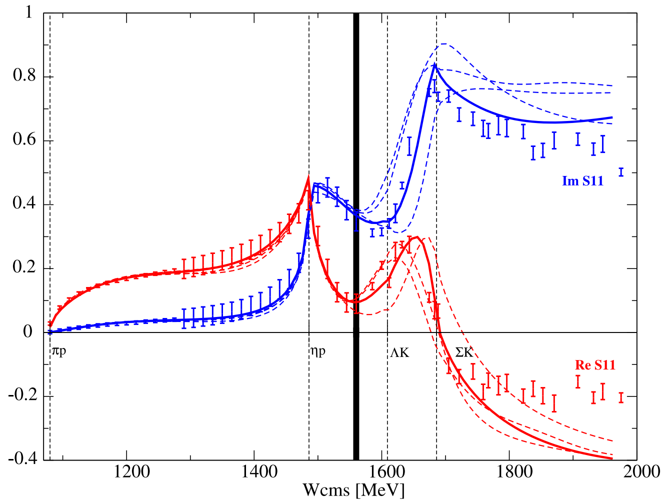

Fig. 2. Real and imaginary part of the S_{11} partial wave amplitude compared with the SAID-data (WI08-analysis). Full curves correspond to the best fit, the dashed ones to fits with slightly worse χ^2_{dof}. The bold vertical line limits the region of the fit, where in the non-fit region single energy values are taken from the SAID-data.

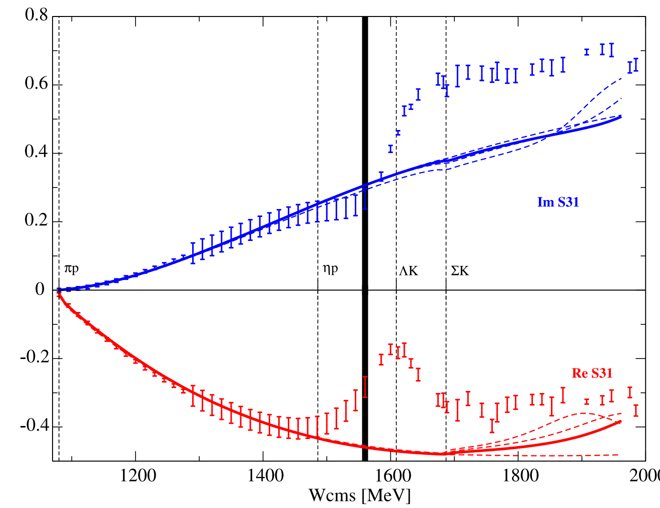

Fig. 3. Real and imaginary part of the S_{31} partial wave amplitude compared with the SAID-data (WI08-analysis). Full curves correspond to the best fit, the dashed ones to fits with slightly worse χ^2_{dof}. The bold vertical line limits the region of the fit, where in the non-fit region single energy values are taken from the SAID-data.

energies an error of 0.030 to the partial wave amplitudes. To some extent this is in agreement with error estimates done in [3], which are motivated by the expectation of pronounced three-body effects above the $\pi\pi N$ threshold. For the best fit, found using the MINUIT library, with a $\chi^2_{\text{dof}} = 1.23$ we obtain the following parameter set (all b_i in GeV^{-1})

$$\begin{aligned}
&\log(\mu_\pi) = +0.924, && b_4 = -0.215, && b_{10} = +1.920,\\
&\log(\mu_K) = +0.581, && b_5 = -0.963, && b_{11} = -0.919,\\
&\log(\mu_\eta) = -0.218, && b_6 = +0.218, && b_0 = -0.768,\\
&b_1 = -0.082, && b_7 = -1.266, && b_D = +0.641,\\
&b_2 = -0.118, && b_8 = +0.609, && b_F = -0.098,\\
&b_3 = -1.890, && b_9 = -0.633. &&
\end{aligned} \tag{11}$$

All parameters are of natural size and LECs agree with the estimates from the SU(3) to SU(2) matching relations provided in [15]. However we are only able to estimate the computational errors on the above parameters within the MIGRAD (MINUIT) minimization procedure, which appear to be negligible.

In Figs. 2 and 3 we present the result of our approach for the S_{11} and S_{31} partial waves. As already seen in earlier publications on the BSE approach with leading-order chiral potential [3], the low-energy region (e.g. $\sqrt{s} < 1.4$ GeV) is reproduced for both isospin 3/2 and 1/2 reasonably well. For the two s-wave scattering lengths, we obtain $a_{1/2} = 145.8 \times 10^{-3}/M_{\pi^+}$ and $a_{3/2} = -91.6 \times 10^{-3}/M_{\pi^+}$, to be compared with the direct extraction of these scattering lengths from the GWU solution, $a_{1/2} = (174.7 \pm 2.2) \times 10^{-3}/M_{\pi^+}$ and $a_{3/2} = (-89.4 \pm 1.7) \times 10^{-3}/M_{\pi^+}$.[1] The theoretically cleanest determination of these observables stems from the analysis of pionic hydrogen and pionic deuterium data based on effective field theory [24], $a_{1/2} = (179.9 \pm 3.6) \times 10^{-3}/M_{\pi^+}$ and $a_{3/2} = (-78.5 \pm 3.2) \times 10^{-3}/M_{\pi^+}$. The description of the πN amplitude at low energies will certainly be improved by a more complete treatment of the Born terms, which is beyond the scope of this Letter. One might also think about constraining the well-known pion–nucleon scattering lengths, e.g. by adopting a matching procedure to the perturbative expansion. However, since we did not put a special weight on the threshold region in our fits, and the overall description of the partial waves seems to work well over a rather broad energy range, we regard the obtained results for the scattering lengths as satisfactory.

Moreover, and more importantly, within the fit region we reproduce the $S_{11}(1535)$, without any use of explicit vector meson resonances or even taking into account the $\pi\pi N$ channels as for example in [2]. At the same time the $S_{31}(1620)$ resonance is not reproduced by our approach, which is in agreement with the current state of knowledge that the first S_{31} resonance does not have a prominent dynamically generated component. To emphasize this we exclude the data on S_{31} and recalculate the χ^2_{dof} for the above parameter set, we end up with $\chi^2_{\text{dof}}(S_{11}) = 0.59$.

At this point one realizes an even more interesting fact: After fixing the S_{11} partial wave in the energy region up to $\sqrt{s} = 1.560$ GeV every curve with minimized χ^2_{dof} possesses a second structure between the $K\Lambda$ and $K\Sigma$ threshold. Obviously this corresponds to the well-known $S_{11}(1650)$ resonance and is predicted here only by demanding a good description in the low-energy and the first resonance region. To some extent this is in agreement with Ref. [3], where the $S_{11}(1650)$ was reproduced in the fit of the phase shifts and inelasticities for the full region of $1.077 < \sqrt{s}/\text{GeV} < 1.946$. While only the leading-order chiral potential was considered there, the authors introduced additional parameters appearing for every loop integral. Apparently these parameters contain some of the information that has to be attributed to neglected terms of higher order in the chiral potential. Additionally, in contrast to our approach this method does not allow to identify the higher partial waves than the s-wave, which might become important for higher energies as emphasized in [5].

In Figs. 4 and 5 we present the modulus of the analytic continuation of $T^{11}_{\pi N}$ into the complex s-plane. In Fig. 4 two poles appear on the (222-111) Riemann sheet, which labels the unphysical Riemann sheet connected to the physical (scattering) axis in the energy region between the third and fourth threshold, i.e. $(M_\eta + m_N)^2 < s < (M_K + m_\Lambda)^2$. For the position of the two poles we extract:

$$W_{1535} = (1.506 - 0.140i)\ \text{GeV},$$

$$W_{1650} = (1.692 - 0.046i)\ \text{GeV}. \tag{12}$$

[1] We thank Ron Workman for providing us with these values.

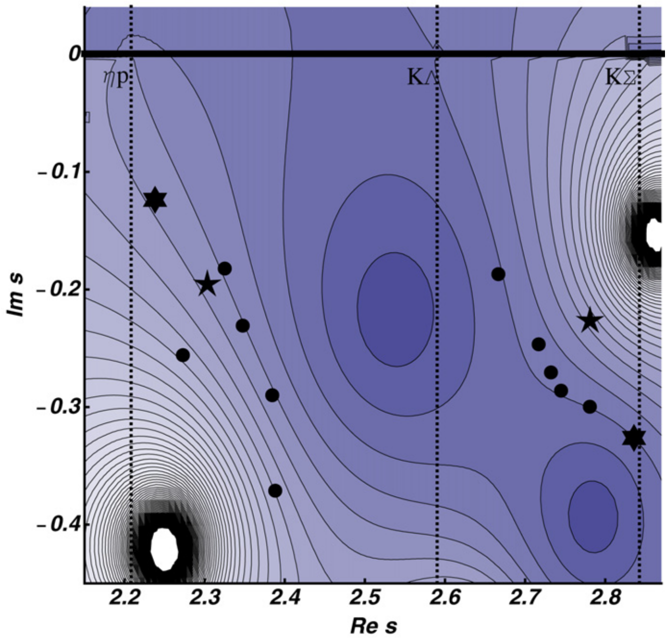

Fig. 4. (222-111) Riemann sheet of the s-plane. The five-star and the six-star correspond to the values obtained in Ref. [4] and Ref. [19], respectively, dots represent results of phenomenological models listed in [25].

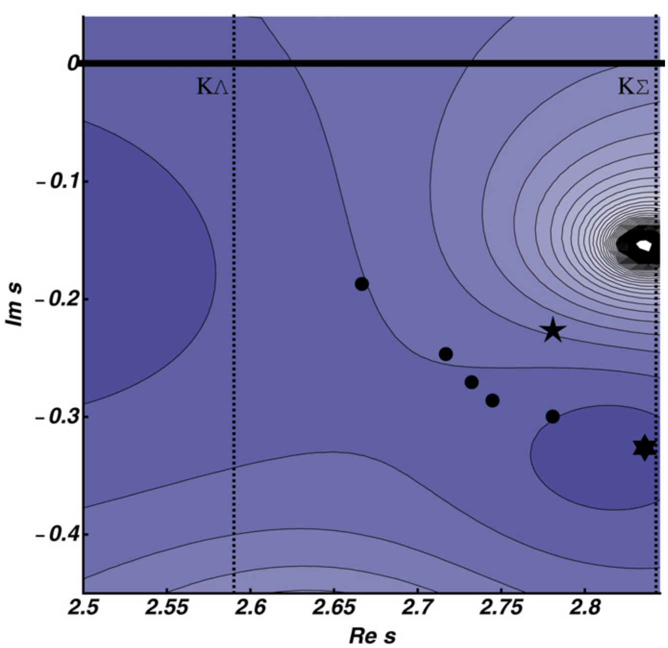

Fig. 5. (2222-11) Riemann sheet of the s-plane. The five-star and the six-star correspond to the values obtained in Ref. [4] and Ref. [19], respectively, dots represent results of phenomenological models listed in [25].

Choosing the (2222-11) Riemann sheet, i.e. the unphysical sheet reached by analytic continuation from the region $(M_K + m_\Lambda)^2 < s < (M_K + m_\Sigma)^2$, see Fig. 5, we obtain one single pole structure, which is located at

$$W_{1650} = (1.682 - 0.042i)\ \text{GeV}. \tag{13}$$

We conclude that the $S_{11}(1650)$ can also be described as a dynamically generated resonance, just like the $S_{11}(1535)$.

Clearly the uncertainty of our predictions grows with increasing energy. As a consequence of the sizeably increased computing time, when fitting the full amplitudes rather than the on-shell approximations to them, we are not able to perform a full error analysis as e.g. done in Ref. [8] for $K^- p$ scattering. Still, we are able to get an indication of the error bands on the partial wave amplitudes. For this we present the second, third and fourth best fits in Figs. 2 and 3 as dashed lines. However the error analysis deserves further studies.

It is further interesting to analyze the structure of these states. To do that, we consider the on-shell scattering matrix in the vicinity of the two poles, where it takes the form

$$T_{ij}^{\text{on}}(s) \simeq \frac{g_i g_j}{s - s_R}, \tag{14}$$

with g_i (g_j) the complex coupling constant for the initial (final) transition of the meson–baryon system. For the $S_{11}(1535)$, we obtain the following ordering

$$|g_{\Lambda K^+}|^2 > |g_{p\eta}|^2 > |g_{\Sigma^+ K^0}|^2 \simeq |g_{n\pi^+}|^2 > |g_{\Sigma^0 K^+}|^2 \simeq |g_{p\pi^0}|^2. \tag{15}$$

We remark that the inequalities between couplings to different πN and $K\Sigma$ channels are mostly due to Clebsch–Gordan coefficients in the associated isospin decompositions. However, isospin symmetry is not exact in the present approach. We find that the largest component is the $K\Lambda$ one and that the coupling to ηN is significantly bigger than the πN ones, in agreement with the empirical fact that the $S_{11}(1535)$ couples dominantly to ηN. The pattern for the $S_{11}(1650)$ looks different,

$$|g_{\Sigma^+ K^0}|^2 > |g_{p\eta}|^2 > |g_{\Sigma^0 K^+}|^2 \simeq |g_{n\pi^+}|^2 > |g_{p\pi^0}|^2 \gg |g_{\Lambda K^+}|^2, \tag{16}$$

i.e. for this resonance the $K\Sigma$ component is dominant and the $K\Lambda$ one is completely negligible, which for instance is indicated by the fact that the pole associated with the $S_{11}(1650)$ is accompanied by a second one on a neighboring sheet, with almost the same coordinates. As for the lower-lying resonance, the coupling to $N\eta$ is bigger than the one to $N\pi$.

4. Summary and outlook

In this Letter, we have analyzed s-wave pion–nucleon scattering in coupled-channel unitarized chiral perturbation theory. The driving kernel includes all local interactions terms of first and second order from the chiral effective Lagrangian. We consider all two-body channels with strangeness zero and charge plus one, but do not include inelasticities generated from three-body $N\pi\pi$ states. The Bethe–Salpeter equation has been solved including the full off-shell dependence of the chiral potential. The parameters are fitted to the real and imaginary part of the S_{11} and the S_{31} partial waves for cms energy below 1.56 GeV. We show that both the $S_{11}(1535)$ and the $S_{11}(1650)$ are generated dynamically, even though the fit range does only include the first resonance. We have also analyzed the structure of these states, which exhibit some marked differences as indicated by the couplings given in Eqs. (15), (16). Quite differently, no resonance is generated in the S_{31} partial wave. We consider this an important step in our program of describing kaon photoproduction from coupled-channel unitarized chiral perturbation theory. Clearly, in the future more work is needed to properly include the Born terms and to perform a systematic error analysis.

Acknowledgements

We thank M. Döring and B. Kubis for a careful reading of the manuscript. One of the authors (M.M.) thanks B. Metsch, S. Kreuzer and H. van Pee for the great assistance with IT issues. Partial financial support by the Helmholtz Association through funds provided to the virtual institute "Spin and strong QCD" (VH-VI-231), by the European Community-Research Infrastructure Integrating Activity "Study of Strongly Interacting Matter" (acronym HadronPhysics2, Grant Agreement No. 227431) under the Seventh Framework Programme of the EU, and by DFG (SFB/TR 16, "Subnuclear Structure of Matter") is gratefully acknowledged.

Appendix A. Couplings

For the channel indices $\{b, j; i, a\}$ corresponding to the process $\phi_i B_a \to \phi_j B_b$ the relevant coupling matrices read

$$
\begin{aligned}
A_{WT}^{b,j;i,a} &= -\frac{1}{4F_jF_i}\langle\lambda^{b\dagger}\big[\big[\lambda^{j\dagger},\lambda^i\big],\lambda^a\big]\rangle,\\
A_{14}^{b,j;i,a} &= -\frac{2}{F_jF_i}\big(b_1\big(\langle\lambda^{b\dagger}\big[\lambda^{j\dagger},\big[\lambda^i,\lambda^a\big]\big]\rangle+\langle\lambda^{b\dagger}\big[\lambda^i,\big[\lambda^{j\dagger},\lambda^a\big]\big]\rangle\big)\\
&\quad + b_2\big(\langle\lambda^{b\dagger}\big\{\lambda^{j\dagger},\big[\lambda^i,\lambda^a\big]\big\}\rangle+\langle\lambda^{b\dagger}\big\{\lambda^i,\big[\lambda^{j\dagger},\lambda^a\big]\big\}\rangle\big)\\
&\quad + b_3\big(\langle\lambda^{b\dagger}\big\{\lambda^{j\dagger},\big\{\lambda^i,\lambda^a\big\}\big\}\rangle+\langle\lambda^{b\dagger}\big\{\lambda^i,\big\{\lambda^{j\dagger},\lambda^a\big\}\big\}\rangle\big)\\
&\quad + 2b_4\langle\lambda^{b\dagger}\lambda^a\rangle\langle\lambda^{j\dagger}\lambda^i\rangle\big),\\
A_{57}^{b,j;i,a} &= -\frac{2}{F_jF_i}\big(b_5\langle\lambda^{b\dagger}\big[\big[\lambda^{j\dagger},\lambda^i\big],\lambda^a\big]\rangle+b_6\langle\lambda^{b\dagger}\big\{\big[\lambda^{j\dagger},\lambda^i\big],\lambda^a\big\}\rangle\\
&\quad + b_7\big(\langle\lambda^{b\dagger}\lambda^{j\dagger}\rangle\langle\lambda^i\lambda^a\rangle+\langle\lambda^{b\dagger}\lambda^i\rangle\langle\lambda^a\lambda^{j\dagger}\rangle\big)\big),\\
A_{811}^{b,j;i,a} &= -\frac{1}{F_jF_i}\big(b_8\big(\langle\lambda^{b\dagger}\big[\lambda^{j\dagger},\big[\lambda^i,\lambda^a\big]\big]\rangle+\langle\lambda^{b\dagger}\big[\lambda^i,\big[\lambda^{j\dagger},\lambda^a\big]\big]\rangle\big)\\
&\quad + b_9\big(\langle\lambda^{b\dagger}\big[\lambda^{j\dagger},\big\{\lambda^i,\lambda^a\big\}\big]\rangle+\langle\lambda^{b\dagger}\big[\lambda^i,\big\{\lambda^{j\dagger},\lambda^a\big\}\big]\rangle\big)\\
&\quad + b_{10}\big(\langle\lambda^{b\dagger}\big\{\lambda^{j\dagger},\big\{\lambda^i,\lambda^a\big\}\big\}\rangle+\langle\lambda^{b\dagger}\big\{\lambda^i,\big\{\lambda^{j\dagger},\lambda^a\big\}\big\}\rangle\big)\\
&\quad + 2b_{11}\langle\lambda^{b\dagger}\lambda^a\rangle\langle\lambda^{j\dagger}\lambda^i\rangle\big),\\
A_{M}^{b,j;i,a} &= -\frac{1}{2F_jF_i}\big(b_D\big(\langle\lambda^{b\dagger}\big\{\big\{\lambda^{j\dagger},\big\{\bar{\mathcal{M}},\lambda^i\big\}\big\},\lambda^a\big\}\rangle\\
&\quad + \langle\lambda^{b\dagger}\big\{\big\{\lambda^i,\big\{\bar{\mathcal{M}},\lambda^{j\dagger}\big\}\big\},\lambda^a\big\}\rangle\big)\\
&\quad + b_F\big(\langle\lambda^{b\dagger}\big[\big\{\lambda^{j\dagger},\big\{\bar{\mathcal{M}},\lambda^i\big\}\big\},\lambda^a\big]\rangle\\
&\quad + \langle\lambda^{b\dagger}\big[\big\{\lambda^i,\big\{\bar{\mathcal{M}},\lambda^{j\dagger}\big\}\big\},\lambda^a\big]\rangle\big)\\
&\quad + 2b_0\big(\langle\lambda^{b\dagger}\lambda^a\rangle\langle\big[\lambda^{j\dagger}\lambda^i\big]\bar{\mathcal{M}}\rangle\big)\big),
\end{aligned}
$$

where λ denote the 3×3 channel matrices (e.g. $\phi = \phi^i\lambda^i$ for the physical meson fields), the F_i are the decay constants of the meson in the respective channel, and $\langle\cdots\rangle$ denotes the trace in flavor space. Moreover, $\bar{\mathcal{M}}$ is obtained from the quark mass matrix $\mathcal{M}$ via the Gell-Mann–Oakes–Renner relations, and given in terms of the meson masses as follows, $\bar{\mathcal{M}} = \frac{1}{2}\operatorname{diag}(M_{K^+}^2 - M_{K^0}^2 + M_{\pi^0}^2, M_{K^0}^2 - M_{K^+}^2 + M_{\pi^0}^2, M_{K^+}^2 + M_{K^0}^2 - M_{\pi^0}^2)$.

References

[1] N. Kaiser, P.B. Siegel, W. Weise, Phys. Lett. B 362 (1995) 23, arXiv:nucl-th/9507036.
[2] T. Inoue, E. Oset, M.J. Vicente Vacas, Phys. Rev. C 65 (2002) 035204, arXiv:hep-ph/0110333.
[3] J. Nieves, E. Ruiz Arriola, Phys. Rev. D 64 (2001) 116008, arXiv:hep-ph/0104307.
[4] M. Döring, C. Hanhart, F. Huang, S. Krewald, U.-G. Meißner, Nucl. Phys. A 829 (2009) 170, arXiv:0903.4337 [nucl-th].
[5] B. Borasoy, P.C. Bruns, U.G. Meissner, R. Nissler, Eur. Phys. J. A 34 (2007) 161, arXiv:0709.3181 [nucl-th].
[6] B. Borasoy, R. Nißler, W. Weise, Eur. Phys. J. A 25 (2005) 79, arXiv:hep-ph/0505239.
[7] J.A. Oller, Eur. Phys. J. A 28 (2006) 63, arXiv:hep-ph/0603134.
[8] B. Borasoy, U.-G. Meißner, R. Nißler, Phys. Rev. C 74 (2006) 055201, arXiv:hep-ph/0606108.
[9] N. Kaiser, P.B. Siegel, W. Weise, Nucl. Phys. A 594 (1995) 325, arXiv:nucl-th/9505043.
[10] E. Oset, A. Ramos, Nucl. Phys. A 635 (1998) 99, arXiv:nucl-th/9711022.
[11] J.A. Oller, E. Oset, A. Ramos, Prog. Part. Nucl. Phys. 45 (2000) 157, arXiv:hep-ph/0002193.
[12] J.A. Oller, U.-G. Meißner, Phys. Lett. B 500 (2001) 263, arXiv:hep-ph/0011146.
[13] M.F.M. Lutz, E.E. Kolomeitsev, Nucl. Phys. A 700 (2002) 193, arXiv:nucl-th/0105042.
[14] U.-G. Meißner, J.A. Oller, Nucl. Phys. A 673 (2000) 311, arXiv:nucl-th/9912026.
[15] M. Mai, P.C. Bruns, B. Kubis, U.-G. Meißner, Phys. Rev. D 80 (2009) 094006, arXiv:0905.2810 [hep-ph].
[16] A. Krause, Helv. Phys. Acta 63 (1990) 3.
[17] M. Frink, U.-G. Meißner, JHEP 0407 (2004) 028, arXiv:hep-lat/0404018.
[18] E.E. Salpeter, H.A. Bethe, Phys. Rev. 84 (1951) 1232.
[19] J. Nieves, E. Ruiz Arriola, Nucl. Phys. A 679 (2000) 57, arXiv:hep-ph/9907469.
[20] T. Fuchs, J. Gegelia, G. Japaridze, S. Scherer, Phys. Rev. D 68 (2003) 056005, arXiv:hep-ph/0302117.
[21] P.C. Bruns, PhD thesis, Univ. Bonn, 2009, http://hss.ulb.uni-bonn.de/diss_online.
[22] R.A. Arndt, W.J. Briscoe, I.I. Strakovsky, R.L. Workman, Phys. Rev. C 74 (2006) 045205, arXiv:nucl-th/0605082.
[23] R. Koch, Nucl. Phys. A 448 (1986) 707.
[24] V. Baru, C. Hanhart, M. Hoferichter, B. Kubis, A. Nogga, D.R. Phillips, arXiv:1003.4444 [nucl-th].
[25] W.M. Yao, et al., Particle Data Group, J. Phys. G 33 (2006) 1.